Anisotropic spin fluctuations in Sr_2RuO_4: Role of spin-orbit coupling and induced strain

Sergio Cobo,[1] Felix Ahn,[2] Ilya Eremin,[2] and Alireza Akbari[1,3,4,*]

[1]*Asia Pacific Center for Theoretical Physics (APCTP), Pohang, Gyeongbuk 790-784, Korea*

[2]*Institut für Theoretische Physik III, Ruhr-Universität Bochum, D-44801 Bochum, Germany*

[3]*Department of Physics, POSTECH, Pohang, Gyeongbuk 790-784, Korea*

[4]*Max Planck POSTECH Center for Complex Phase Materials, POSTECH, Pohang 790-784, Korea*

(Received 22 August 2016; revised manuscript received 6 November 2016; published 14 December 2016)

We analyze the spin anisotropy of the magnetic susceptibility of Sr2RuO4 in the presence of spin-orbit coupling and anisotropic strain using quasi-two-dimensional tight-binding parametrization fitted to the angle-resolved photoemission spectroscopy results. Similar to the previous observations we find the in-plane polarization of the low-**q** magnetic fluctuations and the out-of-plane polarization of the incommensurate magnetic fluctuation at the nesting wave-vector $\mathbf{Q}_1 = (2/3\pi, 2/3\pi)$ but also nearly isotropic fluctuations near $\mathbf{Q}_2 = (\pi/6, \pi/6)$. Furthermore, one finds that, apart from the high-symmetry direction of the tetragonal Brillouin zone, the magnetic anisotropy is maximal, i.e., $\chi^{xx} \neq \chi^{yy} \neq \chi^{zz}$ reflected in the x polarization of the intraband nesting wave-vector $\mathbf{Q}_3 = (\pi/2, \pi)$. This is a consequence of the orbital anisotropy of the t_{2g} orbitals in momentum space. We also study how the magnetic anisotropy evolves in the presence of the strain and find strong Ising-like ferromagnetic fluctuations near the Lifshitz transition for the xy band.

DOI: 10.1103/PhysRevB.94.224507

I. INTRODUCTION

Since its discovery in 1994, strontium ruthenate (Sr_2RuO_4) has been one of the few widely studied triplet superconductors [1,2]. Many experimental results provide indirect evidence for a triplet state with a broken time-reversal symmetry and odd-parity Cooper pairs, although the "smoking gun" experiment is still missing. Among these are the Knight-shift measurements [3,4] that are in agreement with polarized neutron-scattering experiments [5]. There are also indications of the broken time-reversal symmetry by polar Kerr effect measurements [6]. Further studies have been performed to describe the unconventional superconducting state in Sr_2RuO_4 [2,7–15]. Regarding the microscopic mechanism of the Cooper pairing, it is believed to be driven by the spin and charge fluctuations [16–18] where the multiorbital character of the bands plays an important role.

Recent experiments reveal that the transition temperature for the superconducting state in Sr_2RuO_4 can be enhanced locally if pressure is applied [19–21]. A local enhancement of the transition at ~ 1 K was observed near lattice deformations [20], and more specifically, recent developments indicate an enhancement of T_c up to $T_c = 3.4$ K under the application of pressure in the direction of the a axis [22]. In addition, a phase transition from the superconducting state to a spin-density wave state was later predicted for even larger values of strain [23]. This is a remarkable result since Sr_2RuO_4 generally is known to be sensitive to disorder [24].

One of the intriguing complications of Sr_2RuO_4 is its multiorbital and multiband character as the Fermi surface (FS) of this system shows three bands, and very likely not all of the FS pockets are contributing equally to the Cooper pairing [25,26]. For example, it was argued that the two mostly quasi-one-dimensional bands (xz and yz bands) with incommensurate antiferromagnetic (AF) spin and charge fluctuations may be driving superconductivity [17,27]. At the same time, other groups argue in favor of the dominant contribution to the Cooper pairing from the large electron pocket of the xy character. It is centered near the Γ point of the Brillouin zone (BZ) [23] (γ band) and lies close to the Van Hove singularity near the $(\pi,0)$ and $(0,\pi)$ points of the BZ [10,28–30]. Furthermore, the role of orbital versus band description of superconductivity also was discussed [31]. The γ band is believed to mainly be affected by the application of anisotropic strain, consequently, the increase in T_c upon strain is mainly attributed to this band [10]. Further complexity in Sr_2RuO_4 comes from the relatively strong spin-orbit coupling in this system as confirmed by NMR [4], neutron scattering [32], and spin-resolved angle-resolved photoemission spectroscopy (ARPES) [33] experiments. Furthermore, spin-orbit coupling also plays an important role in determining the characteristics of the superconducting state [15,34,35].

In this paper, we study the evolution of the magnetic anisotropy of the spin susceptibility in Sr_2RuO_4 in the presence of spin-orbit coupling and anisotropic strain using the tight-binding model fitted to the available ARPES results [36]. We compute the components of the spin susceptibility to obtain the full structure of the spin anisotropy within the itinerant description for the Hubbard-Hund type of interaction model. Our results show clear anisotropy of the different components of the spin susceptibility enhanced by the interaction effects. Furthermore, we analyze how this anisotropy changes upon the strain application.

II. MODEL AND METHODS

The crystal field of the O^{2-} oxygen ions breaks the degeneracy of the $4d$ states of Ru^{4+} into two subshells, the threefold t_{2g} orbitals and the twofold e_g orbitals. The orbital character of the FS is dominated by the t_{2g} subshell which has a lower energy because the orbitals' lobes point between the oxygen ions in contrast to the e_g orbitals. The system is not particle-hole symmetric and has a relatively

*alireza@apctp.org

low effective bandwidth [37,38]. In other words, there is one additional electron in the half-filled t_{2g} shell or four electrons per site [39]. Recently, there have been detailed first-principles calculations on the electronic structure by self-consistent *GW* calculations [38,40]. Moreover, a series of studies investigates the correlation effects of these materials [41–44]. Later, detailed ARPES measurements [45] and de Haas–van Alphen experiments [46,47] were shown to be consistent with local-density approximation (LDA) bands [48,49], renormalized due to correlations.

As a starting point, we use the effective three orbital model including the t_{2g} orbital manifold,

$$H_0(\mathbf{k}) = \sum_{\mathbf{k},\nu,\sigma} \epsilon_\nu(\mathbf{k}) d^\dagger_{\mathbf{k}\nu\sigma} d_{\mathbf{k}\nu\sigma}, \tag{1}$$

where orbital indices are given by $\nu = xz, yz, xy$ with spinor $\psi^\dagger(\mathbf{k}\sigma) = (d^\dagger_{\mathbf{k},xz,\sigma}, d^\dagger_{\mathbf{k},yz,\sigma}, d^\dagger_{\mathbf{k},xy,\bar{\sigma}})$, where $\mathbf{k}$ and σ ($\bar{\sigma} = -\sigma$) represent momentum and spin, respectively. The electronic dispersion is defined with the help of tight-binding parametrization,

$$\begin{aligned} \epsilon_{xz/yz}(\mathbf{k}) &= -2t_{1/2}\cos k_x - 2t_{2/1}\cos k_y, \\ \epsilon_{xy}(\mathbf{k}) &= -2t_3(\cos k_x + \cos k_y) - 4t_4 \cos k_x \cos k_y \\ &\quad - 2t_5(\cos 2k_x + \cos 2k_y), \end{aligned} \tag{2}$$

and the hopping parameters [$t_1 = 88$, $t_2 = 9$, $t_3 = 80$, $t_4 = 40$, $t_5 = 5$, $\mu = 109$ (all in meV)] are fitted to the available ARPES experiments [36].

In addition, we include the on-site spin-orbit coupling [26,34,35] $\mathcal{H}_{\rm SOC} = \lambda \mathbf{S}\cdot\mathbf{L}$, where $\mathbf{S}$ and $\mathbf{L}$ are the spin and angular momentum operators. Written in terms of the t_{2g} manifold $(d^\dagger_{xz\uparrow}, d^\dagger_{yz\uparrow}, d^\dagger_{xy\downarrow}, d^\dagger_{xz\downarrow}, d^\dagger_{yz\downarrow}, d^\dagger_{xy\uparrow})$ the spin-orbit coupling acquires the following form [35]:

$$H_{\rm SOC} = \frac{1}{2}\begin{pmatrix} 0 & i\lambda & i\lambda & 0 & 0 & 0 \\ -i\lambda & 0 & -\lambda & 0 & 0 & 0 \\ -i\lambda & -\lambda & 0 & 0 & 0 & 0 \\ 0 & 0 & 0 & 0 & -i\lambda & \lambda \\ 0 & 0 & 0 & i\lambda & 0 & -i\lambda \\ 0 & 0 & 0 & \lambda & i\lambda & 0 \end{pmatrix}, \tag{3}$$

and we employ $\lambda = 35$ meV [36]. The diagonalization of the combined Hamiltonian $\mathcal{H} = \mathcal{H}_0 + \mathcal{H}_{\rm SOC}$ yields the electronic band structure that shows two electronlike FS pockets around Γ and a holelike FS pocket around the M point of the BZ [36]. The resulting Fermi-surface topology and band structure are shown in the insets of Figs. 1(a) and 1(b), respectively. The interaction part of the Hamiltonian contains the on-site Hubbard-Hund-type interactions, written in terms of Hubbard intra-(U) and inter-(U') orbital terms as well as the residual Hund coupling J and pair hopping J',

$$\begin{aligned} \mathcal{H}_{\rm int} &= \sum_{l,\nu,\sigma} \frac{U}{2} d^\dagger_{l\nu\sigma} d^\dagger_{l\nu\bar{\sigma}} d_{l\nu\bar{\sigma}} d_{l\nu\sigma} \\ &\quad + \sum_{l,\nu\neq\nu',\sigma\sigma'} \frac{U'}{2} d^\dagger_{l\nu\sigma} d^\dagger_{l\nu'\sigma'} d_{l\nu'\sigma'} d_{l\nu\sigma} \end{aligned}$$

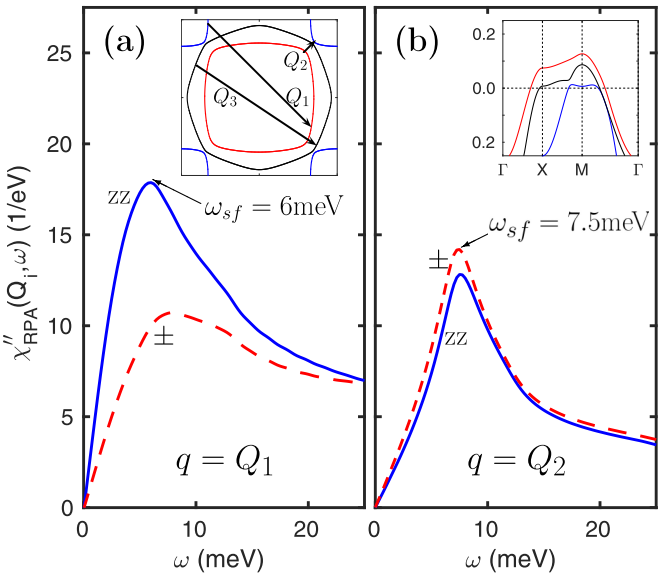

FIG. 1. Calculated imaginary part of the longitudinal and transverse components of the random-phase approximation (RPA) spin susceptibility at the antiferromagnetic wave-vectors (a) $\mathbf{Q}_1 = (2\pi/3, 2\pi/3)$ and (b) $\mathbf{Q}_2 = (\pi/6, \pi/6)$. The insets show the Fermi-surface topology with corresponding nesting wave vectors as the electronic dispersion along high-symmetry lines, respectively.

$$\begin{aligned} &+ \sum_{l,\nu\neq\nu',\sigma\sigma'} \frac{J}{2} d^\dagger_{l\nu\sigma} d^\dagger_{l\nu'\sigma'} d_{l\nu\sigma'} d_{l\nu'\sigma} \\ &+ \sum_{l,\nu\nu',\sigma} \frac{J'}{2} d^\dagger_{l\nu\sigma} d^\dagger_{l\nu\bar{\sigma}} d_{l\nu'\bar{\sigma}} d_{l\nu'\sigma}, \end{aligned} \tag{4}$$

here l runs over the lattice sites.

The physical components of the spin susceptibility are given by

$$\chi_0^{uv}(\mathbf{q}, i\Omega) = \frac{-T}{4N} \sum_{\substack{\mathbf{k}, i\omega_n \\ p=q, s=t}} \sigma^u_{\gamma\delta}\sigma^v_{\alpha\beta} G^{\mathbf{k}, i\omega_n}_{qs,\beta\gamma} G^{\mathbf{k}', i\omega_n + i\Omega}_{tp,\delta\alpha}, \tag{5}$$

where $\mathbf{k}' = \mathbf{k} + \mathbf{q}$ and $\sigma^{u=x,y,z}$ are the Pauli matrices. Here, q, p, s, t and $\alpha, \beta, \gamma, \delta$ are the orbital and the spin indices, respectively. The Green's function is defined by

$$G^{\mathbf{k}, i\omega_n}_{ss',\sigma\sigma'} = -\int_0^\beta d\tau\, e^{i\omega\tau} \langle T_\tau d_{\mathbf{k},s\sigma}(\tau) d^\dagger_{\mathbf{k},s'\sigma'}(0)\rangle,$$

where the transformation from the orbital and the spin basis to the band pseudospin basis is performed by substitution of

$$G^{\mathbf{k},\tau}_{ss',\sigma\sigma'} = \sum_i a_{s\sigma}(i,\mathbf{k}) a^*_{s'\sigma'}(i,\mathbf{k}) G_i(\mathbf{k},\tau). \tag{6}$$

Here, $a_{s\sigma}(i,\mathbf{k})$ is the matrix element that connects band (i) and orbital (s). Performing the Matsubara frequency sum over $i\omega_n \longrightarrow \omega + i0^+$, the expression for the components of the bare susceptibility in the multiorbital case is given

by

$$\chi_0^{uv}(\mathbf{q},\omega) = \sum_{ij,\mathbf{k}} \left[\eta_{ij;\mathbf{k}\mathbf{k}'}^{uv}\right] \frac{f\left(E_i^{\mathbf{k}}\right) - f\left(E_j^{\mathbf{k}'}\right)}{E_j^{\mathbf{k}'} - E_i^{\mathbf{k}} + \omega + i0^+}, \tag{7}$$

here the anisotropy of the susceptibility enters through the orbital and spin-dressing factor,

$$\left[\eta_{ij;\mathbf{k}\mathbf{k}'}^{uv}\right] = \sigma_{\alpha\beta}^{u}\sigma_{\gamma\delta}^{v} a_{t\beta}(i,\mathbf{k}) a_{s\gamma}^{*}(i,\mathbf{k}) a_{s\delta}(j,\mathbf{k}') a_{t\alpha}^{*}(j,\mathbf{k}'),$$

that implies summation over the repeated indexes.

On the diagrammatic level, the bare susceptibility can also be written as

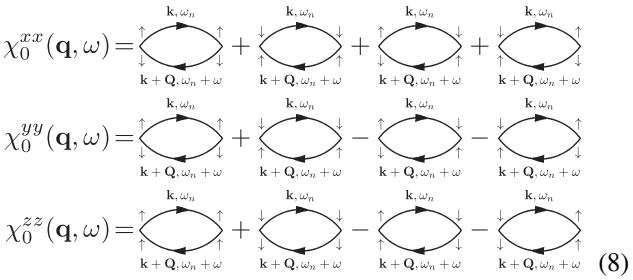

(8)

where we define the following notation for the diagrams:

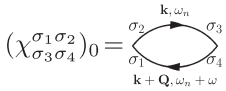

(9)

This allows us to write each component within short-hand notation as

$$\begin{aligned}
\chi_0^{xx}(\mathbf{q},\omega) &= \left(\chi_{\uparrow\downarrow}^{\uparrow\downarrow} + \chi_{\downarrow\uparrow}^{\downarrow\uparrow} + \chi_{\downarrow\uparrow}^{\uparrow\downarrow} + \chi_{\uparrow\downarrow}^{\downarrow\uparrow}\right)_0, \\
\chi_0^{yy}(\mathbf{q},\omega) &= \left(\chi_{\uparrow\downarrow}^{\uparrow\downarrow} + \chi_{\downarrow\uparrow}^{\downarrow\uparrow} - \chi_{\downarrow\uparrow}^{\uparrow\downarrow} - \chi_{\uparrow\downarrow}^{\downarrow\uparrow}\right)_0, \\
\chi_0^{zz}(\mathbf{q},\omega) &= \left(\chi_{\uparrow\uparrow}^{\uparrow\uparrow} + \chi_{\downarrow\downarrow}^{\downarrow\downarrow} - \chi_{\downarrow\downarrow}^{\uparrow\uparrow} - \chi_{\uparrow\uparrow}^{\downarrow\downarrow}\right)_0.
\end{aligned} \tag{10}$$

Again, for the physical part of the susceptibility, the summation of indices is implied. Here for zero spin-orbit coupling $\lambda = 0$, the first two bubbles of each component have the same value, whereas the last two bubbles of each component vanish, ensuring the $O(3)$ symmetry of the system. If spin-orbit coupling acts only among the d_{xz} and d_{yz} orbitals, the only term is $\lambda S_z L_z$, and it already leads to a splitting of the transverse and longitudinal parts of the susceptibility $\chi_0^{xx}(\mathbf{q},\omega) = \chi_0^{yy}(\mathbf{q},\omega) \neq \chi_0^{zz}(\mathbf{q},\omega)$. However, if spin-orbit coupling acts among at least one additional orbital, the transverse components χ_0^{xx} (χ_0^{yy}) differ due to the term $\lambda(S_+L_- + S_-L_+)$, implying full spin anisotropy in the entire BZ $\chi_0^{xx}(\mathbf{q},\omega) \neq \chi_0^{yy}(\mathbf{q},\omega) \neq \chi_0^{zz}(\mathbf{q},\omega)$.

The diagrammatic treatment for the random-phase approximation needs to be performed separately for the longitudinal (zz) and the transverse (xx, yy) components of the spin susceptibility. In particular, one finds

$$\begin{pmatrix} \chi_{\uparrow\downarrow}^{\uparrow\downarrow} & \chi_{\uparrow\downarrow}^{\downarrow\uparrow} \\ \chi_{\downarrow\uparrow}^{\uparrow\downarrow} & \chi_{\downarrow\uparrow}^{\downarrow\uparrow} \end{pmatrix}_{\mathrm{RPA}} = \left[\mathbb{I} - \begin{pmatrix} \chi_{\uparrow\downarrow}^{\uparrow\downarrow} & \chi_{\uparrow\downarrow}^{\downarrow\uparrow} \\ \chi_{\downarrow\uparrow}^{\uparrow\downarrow} & \chi_{\downarrow\uparrow}^{\downarrow\uparrow} \end{pmatrix}_0 \begin{pmatrix} U_{\uparrow\downarrow}^{\uparrow\downarrow} & 0 \\ 0 & U_{\downarrow\uparrow}^{\downarrow\uparrow} \end{pmatrix}\right]^{-1} \times \begin{pmatrix} \chi_{\uparrow\downarrow}^{\uparrow\downarrow} & \chi_{\uparrow\downarrow}^{\downarrow\uparrow} \\ \chi_{\downarrow\uparrow}^{\uparrow\downarrow} & \chi_{\downarrow\uparrow}^{\downarrow\uparrow} x \end{pmatrix}_0, \tag{11}$$

and

$$\begin{pmatrix} \chi_{\uparrow\uparrow}^{\uparrow\uparrow} & \chi_{\uparrow\uparrow}^{\downarrow\downarrow} \\ \chi_{\downarrow\downarrow}^{\uparrow\uparrow} & \chi_{\downarrow\downarrow}^{\downarrow\downarrow} \end{pmatrix}_{\mathrm{RPA}} = \left[\mathbb{I} - \begin{pmatrix} \chi_{\uparrow\uparrow}^{\uparrow\uparrow} & \chi_{\uparrow\uparrow}^{\downarrow\downarrow} \\ \chi_{\downarrow\downarrow}^{\uparrow\uparrow} & \chi_{\downarrow\downarrow}^{\downarrow\downarrow} \end{pmatrix}_0 \begin{pmatrix} U_{\uparrow\uparrow}^{\uparrow\uparrow} & U_{\downarrow\downarrow}^{\uparrow\uparrow} \\ U_{\uparrow\uparrow}^{\downarrow\downarrow} & U_{\downarrow\downarrow}^{\downarrow\downarrow} \end{pmatrix}\right]^{-1} \times \begin{pmatrix} \chi_{\uparrow\uparrow}^{\uparrow\uparrow} & \chi_{\uparrow\uparrow}^{\downarrow\downarrow} \\ \chi_{\downarrow\downarrow}^{\uparrow\uparrow} & \chi_{\downarrow\downarrow}^{\downarrow\downarrow} \end{pmatrix}_0. \tag{12}$$

Here, each entry of the matrix is a tensor with four orbital indices $\{pqst\}$, and the summation over orbital indices for the physical part of the susceptibility has to be performed at the end. Furthermore, the matrix equations in the spin space can be decoupled by applying the similarity transformation $S = (\sigma^x + \sigma^z)/\sqrt{2}$, which yields four decoupled equations. The three equations that correspond to the spin susceptibility are written below,

$$\chi_{\mathrm{RPA}}^{uu}(\mathbf{q},\omega) = \left[1 - \chi_0^{uu}(\mathbf{q},\omega)U_s\right]^{-1} \chi_0^{uu}(\mathbf{q},\omega), \tag{13}$$

where $uu = xx, yy, zz$. Furthermore, $U_s \equiv U_{\uparrow\uparrow}^{\uparrow\uparrow} - U_{\downarrow\downarrow}^{\uparrow\uparrow} = U_{\uparrow\downarrow}^{\uparrow\downarrow}$ contains the Hubbard-type on-site interactions U, J, and $U' = U - 2J$. In particular, U (U') is the intra- (inter-) orbital Coulomb repulsion, and J represents Hund's coupling. The tensor U_s is given by

$$\begin{aligned}
(U_s)_{aa}^{aa} &= U, \qquad (U_s)_{ab}^{ab} = U', \\
(U_s)_{bb}^{aa} &= J, \qquad (U_s)_{ba}^{ab} = J.
\end{aligned} \tag{14}$$

III. NUMERICAL RESULTS

The well-known fact of the electronic structure of Sr_2RuO_4 is the nesting of the quasi-one-dimensional xz and yz bands at the incommensurate wave-vector $\mathbf{Q}_1$ [16]. In the inelastic neutron scattering this nesting yields the incommensurate magnetic fluctuations peaked at $\omega_{sf} = 6$ meV, which are polarized along the z direction. The parameters of the noninteracting Hamiltonian are fixed in our case by the fit to the ARPES experiments [36]. Thus we employ $U = 1.5t_3$ and $J = 0.25U$ to reproduce the frequency position of 6 meV of the incommensurate spin fluctuations at $\mathbf{Q}_1$ in the longitudinal response as shown in Fig. 1(a). Note that this value of U should be considered as some effective one as we are using the ARPES-based tight-binding parameters and not the original LDA values. At the next step we find that the transverse fluctuations are peaked at more or less the same frequency but appear to be with a factor 2 smaller intensity, which again agrees very well with the neutron-scattering data [32]. Analyzing each component of the RPA susceptibility in detail, we find that the easy-axis (z) polarization of the incommensurate AF fluctuation at $\mathbf{Q}_1$ occurs due to the dominant interband nesting of the xz (yz) bands.

As is generally believed that the pure AF fluctuation cannot be responsible for the triplet character of the Cooper pairing, we have analyzed the behavior of the spin response in the entire BZ. In particular, in Fig. 2, we show the results of the RPA physical susceptibility and its anisotropy in the first BZ. In addition to the incommensurate AF fluctuations at $\mathbf{Q}_1$, we find dispersing magnetic excitation, peaked at much smaller momentum $\mathbf{Q}_2 = (\pi/6, \pi/6)$ (see Fig. 3). This wave vector refers to the interband nesting of the xy- and (xy/yz)-based

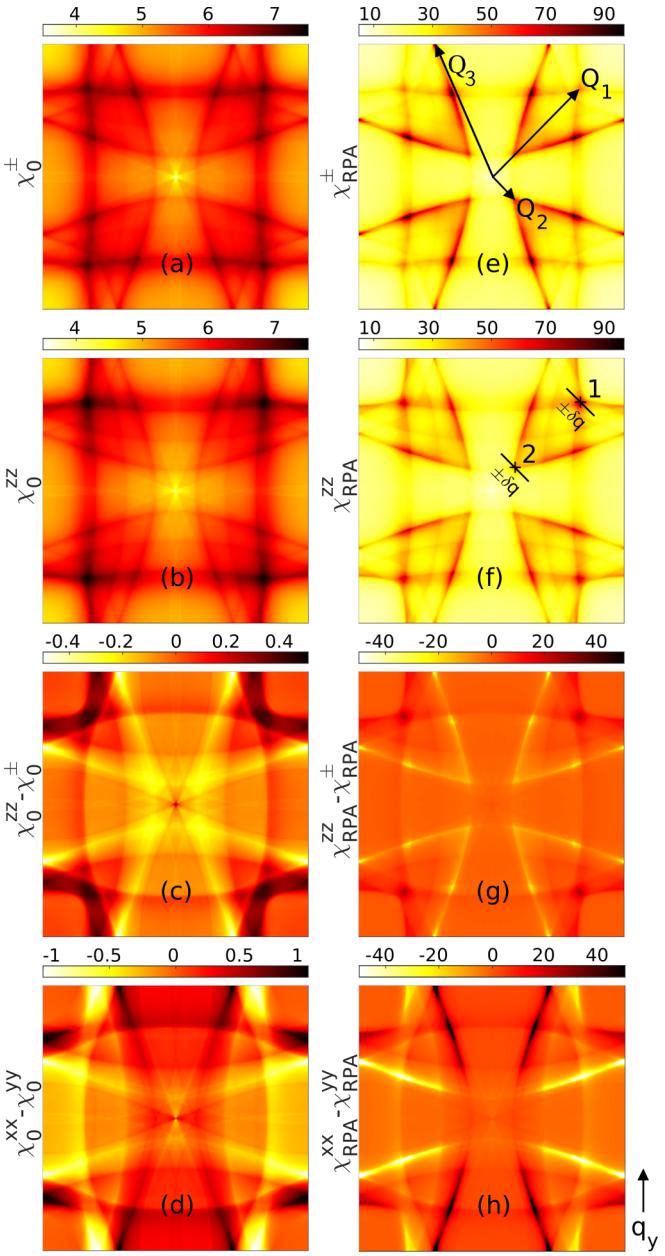

FIG. 2. Calculated real parts of (a)–(d) the bare and (e)–(h) the RPA physical spin susceptibilities as a function of $\mathbf{q}$ in the static limit $\omega = 0$ for the longitudinal and transverse components. The units are given in π/a in the range of $[-1,1]$. The arrows in panel (e) show the corresponding nesting wave vectors from Fig. 1.

bands as shown in the inset of Fig. 1. These small-$\mathbf{q}$ excitations also were observed previously [50]. These excitations appear to be weakly anisotropic as shown in Fig. 1(b) and for the value of the interactions employed are peaked at energies of about 7.5 meV. Surprisingly their intensity appears to have a similar magnitude as the excitations at $\mathbf{Q}_1$, which could be a result of the stronger nesting feature of the two-dimensional tight-binding parametrization, employed in the ARPES experiment [36]. We expect these fluctuations to become less pronounced once the weak-k_z dispersion is included.

Another interesting feature we see from Fig. 2 is that maximal magnetic anisotropy of the spin fluctuations in Sr_2RuO_4

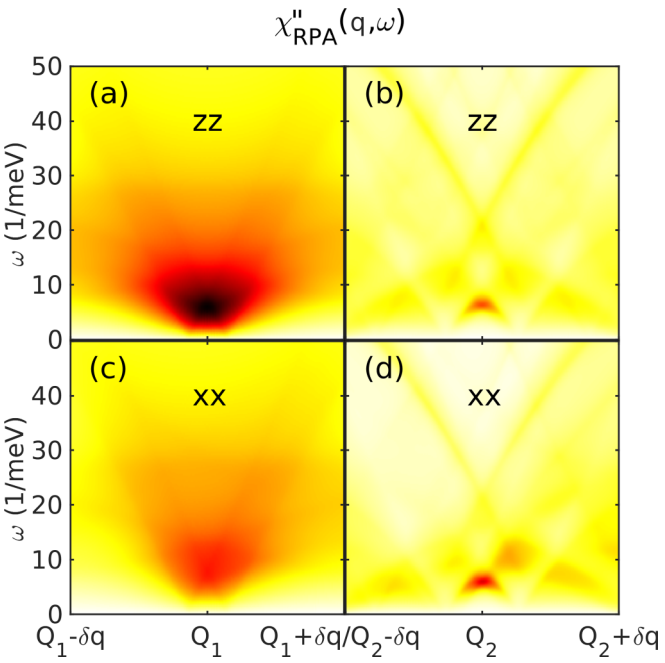

FIG. 3. Calculated frequency and momentum dependencies of the imaginary parts of χ^{zz}_{RPA} and χ^{xx}_{RPA} near (a) and (c) $\mathbf{Q}_1$ and (b) and (d) $\mathbf{Q}_2$. The two straight lines, defined by the end points of $(\mathbf{Q}_i - \delta q, \mathbf{Q}_i + \delta q)$, $i = 1,2$, are visualized in Fig. 2(f).

away from the high-symmetry directions. The components of the susceptibility remain anisotropic, and in general away from any high-symmetry points, one observes $\chi^{xx} \neq \chi^{yy} \neq \chi^{zz}$. In particular, $\chi^{zz} > \chi^{xx/yy}$ near the M point, yet $\chi^{xx} < \chi^{yy}$ and $\chi^{xx} > \chi^{yy}$ around the X and Y points, respectively, implying a breaking of the in-plane symmetry of the spin susceptibility. This anisotropy is particularly pronounced for the intraband nesting of the xy band at the wave-vector $\mathbf{Q}_3 \approx (\pi/2,\pi)$ as shown in Fig. 4(a). Note that such an anisotropy of the spin fluctuations is related to the spin-orbit coupling that transfers the highly anisotropic orbital character t_{2g} orbitals to the spin subspace. Theses anisotropies should also be seen in the dispersion of both excitations at $\mathbf{Q}_1$ and $\mathbf{Q}_2$, which we present in Fig. 4.

Observe that this anisotropy should become strongly visible once the anisotropic strain $\epsilon_{xx} = -\epsilon_{yy} < 0$ is applied. In the following we include its effect on the electronic structure via anisotropic intraorbital hopping parameters along the x and y directions of the kinetic part of the Hamiltonian (t_1–t_3, and t_5) as $t_i \longrightarrow t_i + \eta_{\mathbf{b}}\delta t_i$ with $\eta_{\mathbf{b}} = \pm 1$ for $\mathbf{b} = \hat{x}/\hat{y}$ and $\delta t \propto -\epsilon_{xx} > 0$ such that it breaks the C_4 symmetry of the system especially for the xy orbital, similar to Ref. [22]. We find that for 2.65% strain the Fermi surface of the xy band touches the Van Hove singularity at the Y point.

Although all FS pockets are just C_2 symmetric under strain, the larger electron band around Γ is distorted significantly [23] and is responsible for the sharp increase in states at the Fermi level, which can be seen in Fig. 4(b). For strain values close to the Van Hove singularity, we find that the dominating peak of the real part of the magnetic response shifts appears at $\mathbf{q} = 0$ as a result of the Van Hove singularity crossing the Fermi level with spin polarization along the y direction.

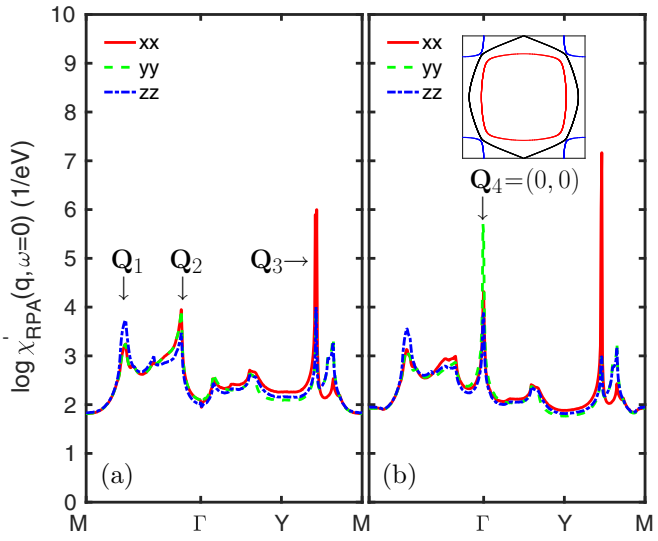

FIG. 4. Calculated real part of the RPA spin susceptibility along high-symmetry directions of the BZ with nesting wave vectors at $\mathbf{Q}_1$–$\mathbf{Q}_3$. The anisotropy of the longitudinal and transverse components results from (a) spin-orbit coupling and results from (b) spin-orbit coupling including anisotropic strain; the anisotropy at the dominating peak at $\mathbf{Q}_4$ (Γ) is $yy > xx > zz$. The inset shows the Fermi-surface topology with Van Hove singularity at the Y point.

IV. DISCUSSION AND CONCLUSION

To conclude we study the anisotropy of the spin fluctuations in Sr_2RuO4 in the presence of spin-orbit coupling and anisotropic strain using quasi-two-dimensional tight-binding parametrization fitted to the ARPES results. Similar to the previous observations we find the in-plane polarization of the low-$\mathbf{q}$ magnetic fluctuations and the out-of-plane polarization of the incommensurate magnetic fluctuation at the nesting wave-vector $\mathbf{Q}_1 = (2/3\pi, 2/3\pi)$. Most importantly we also find strong fluctuations near the much smaller wave-vector $\mathbf{Q}_2 = (\pi/6, \pi/6)$ with weak anisotropy and intraband nesting $\mathbf{Q}_3 \approx (\pi/2, \pi)$ with Ising-type polarization. Furthermore, one finds that apart from the high-symmetry direction of the tetragonal Brillouin zone the magnetic anisotropy is maximal, i.e., $\chi^{xx} \neq \chi^{yy} \neq \chi^{zz}$. This is a consequence of the orbital anisotropy of the xz and yz orbitals in momentum space. We also study how the magnetic anisotropy evolves in the presence of the strain and finds strong Ising-like ferromagnetic fluctuations which appear when the xy band touches the Van Hove point at the Y point of the BZ.

Overall we find that the spin-orbit coupling introduces substantial magnetic anisotropy of the continuum of the spin fluctuations. Its impact on the Cooper pairing still needs to be clarified in a separate study. However, we expect that it should influence significantly the Cooper-pairing instabilities in Sr_2RuO_4 in a somewhat similar fashion as it occurs once the spin-rotational symmetry is broken due to the presence of the magnetic phase [51].

ACKNOWLEDGMENTS

We acknowledge helpful discussions with B. Andersen, M. Braden, M. M. Korshunov, P. Hirschfeld, A. Romer, and P. Thalmeier. S.C. and A.A. wish to acknowledge the Korea Ministry of Education, Science and Technology, Gyeongsangbuk-Do, and Pohang City for Independent Junior Research Groups at the Asia Pacific Center for Theoretical Physics. The work by A.A. was supported through the NRF funded by the MSIP of Korea (Grant No. 2015R1C1A1A01052411) and by the Max Planck POSTECH/KOREA Research Initiative (Grant No. 2011-0031558) programs through the NRF funded by the MSIP of Korea.

[1] Y. Maeno, H. Hashimoto, K. Yoshida, S. Nishizaki, T. Fujita, J. G. Bednorz, and F. Lichtenberg, Nature (London) **372**, 532 (1994).
[2] A. P. Mackenzie and Y. Maeno, Rev. Mod. Phys. **75**, 657 (2003).
[3] K. Ishida, H. Mukuda, Y. Kitaoka, K. Asayama, Z. Q. Mao, Y. Mori, and Y. Maeno, Nature (London) **396**, 658 (1998).
[4] K. Ishida, M. Manago, T. Yamanaka, H. Fukazawa, Z. Q. Mao, Y. Maeno, and K. Miyake, Phys. Rev. B **92**, 100502 (2015).
[5] J. A. Duffy, S. M. Hayden, Y. Maeno, Z. Mao, J. Kulda, and G. J. McIntyre, Phys. Rev. Lett. **85**, 5412 (2000).
[6] J. Xia, Y. Maeno, P. T. Beyersdorf, M. M. Fejer, and A. Kapitulnik, Phys. Rev. Lett. **97**, 167002 (2006).
[7] Y. Maeno, S. Kittaka, T. Nomura, S. Yonezawa, and K. Ishida, J. Phys. Soc. Jpn. **81**, 011009 (2011).
[8] F. Kidwingira, J. D. Strand, D. J. Van Harlingen, and Y. Maeno, Science **314**, 1267 (2006).
[9] K. D. Nelson, Z. Q. Mao, Y. Maeno, and Y. Liu, Science **306**, 1151 (2004).
[10] Q. H. Wang, C. Platt, Y. Yang, C. Honerkamp, F. C. Zhang, W. Hanke, T. M. Rice, and R. Thomale, Europhys. Lett. **104**, 17013 (2013).
[11] J.-W. Huo and F.-C. Zhang, Phys. Rev. B **87**, 134501 (2013).
[12] C. Rastovski, C. D. Dewhurst, W. J. Gannon, D. C. Peets, H. Takatsu, Y. Maeno, M. Ichioka, K. Machida, and M. R. Eskildsen, Phys. Rev. Lett. **111**, 087003 (2013).
[13] Y. Maeno, T. M. Rice, and M. Sigrist, Phys. Today **54**(1), 42 (2001).
[14] A. Akbari and P. Thalmeier, Phys. Rev. B **88**, 134519 (2013).
[15] J. F. Annett, G. Litak, B. L. Györffy, and K. I. Wysokiński, Phys. Rev. B **73**, 134501 (2006).
[16] I. Eremin, D. Manske, S. Ovchinnikov, and J. Annett, Ann. Phys. (NY) **13**, 149 (2004).
[17] S. Raghu, A. Kapitulnik, and S. A. Kivelson, Phys. Rev. Lett. **105**, 136401 (2010).
[18] M. Tsuchiizu, Y. Yamakawa, S. Onari, Y. Ohno, and H. Kontani, Phys. Rev. B **91**, 155103 (2015).
[19] H. Taniguchi, K. Nishimura, S. K. Goh, S. Yonezawa, and Y. Maeno, J. Phys. Soc. Jpn. **84**, 014707 (2014).
[20] Y. A. Ying, N. E. Staley, Y. Xin, K. Sun, X. Cai, D. Fobes, T. J. Liu, Z. Q. Mao, and Y. Liu, Nat. Commun. **4**, 2596 (2013).

[21] C. W. Hicks, D. O. Brodsky, E. A. Yelland, A. S. Gibbs, J. A. N. Bruin, M. E. Barber, S. D. Edkins, K. Nishimura, S. Yonezawa, Y. Maeno, and A. P. Mackenzie, Science **344**, 283 (2014).
[22] A. Steppke, L. Zhao, M. E. Barber, T. Scaffidi, F. Jerzembeck, H. Rosner, A. S. Gibbs, Y. Maeno, S. H. Simon, A. P. Mackenzie, and C. W. Hicks, arXiv:1604.06669.
[23] Y. C. Liu, F. C. Zhang, T. M. Rice, and Q. H. Wang, arXiv:1604.06666.
[24] A. P. Mackenzie, R. K. W. Haselwimmer, A. W. Tyler, G. G. Lonzarich, Y. Mori, S. Nishizaki, and Y. Maeno, Phys. Rev. Lett. **80**, 161 (1998).
[25] D. F. Agterberg, T. M. Rice, and M. Sigrist, Phys. Rev. Lett. **78**, 3374 (1997).
[26] T. Scaffidi, J. C. Romers, and S. H. Simon, Phys. Rev. B **89**, 220510 (2014).
[27] I. A. Firmo, S. Lederer, C. Lupien, A. P. Mackenzie, J. C. Davis, and S. A. Kivelson, Phys. Rev. B **88**, 134521 (2013).
[28] T. Nomura and K. Yamada, J. Phys. Soc. Jpn. **69**, 3678 (2000).
[29] Y. Yanase and M. Ogata, J. Phys. Soc. Jpn. **72**, 673 (2003).
[30] T. Nomura and K. Yamada, J. Phys. Soc. Jpn. **71**, 404 (2002).
[31] V. P. Mineev, Phys. Rev. B **89**, 134519 (2014).
[32] M. Braden, P. Steffens, Y. Sidis, J. Kulda, P. Bourges, S. Hayden, N. Kikugawa, and Y. Maeno, Phys. Rev. Lett. **92**, 097402 (2004).
[33] C. N. Veenstra, Z.-H. Zhu, M. Raichle, B. M. Ludbrook, A. Nicolaou, B. Slomski, G. Landolt, S. Kittaka, Y. Maeno, J. H. Dil, I. S. Elfimov, M. W. Haverkort, and A. Damascelli, Phys. Rev. Lett. **112**, 127002 (2014).
[34] K. K. Ng and M. Sigrist, Europhys. Lett. **49**, 473 (2000).
[35] I. Eremin, D. Manske, and K. H. Bennemann, Phys. Rev. B **65**, 220502 (2002).
[36] V. B. Zabolotnyy, D. V. Evtushinsky, A. A. Kordyuk, T. K. Kim, E. Carleschi, B. P. Doyle, R. Fittipaldi, M. Cuoco, A. Vecchione, and S. V. Borisenko, J. Electron Spectrosc. Relat. Phenom. **191**, 48 (2013).
[37] L. de' Medici, J. Mravlje, and A. Georges, Phys. Rev. Lett. **107**, 256401 (2011).
[38] J. Mravlje, M. Aichhorn, T. Miyake, K. Haule, G. Kotliar, and A. Georges, Phys. Rev. Lett. **106**, 096401 (2011).
[39] A. Georges, L. de' Medici, and J. Mravlje, Annu. Rev. Condens. Matter Phys. **4**, 137 (2013).
[40] S. Ryee, S. W. Jang, H. Kino, T. Kotani, and M. J. Han, Phys. Rev. B **93**, 075125 (2016).
[41] T. T. Tran, T. Mizokawa, S. Nakatsuji, H. Fukazawa, and Y. Maeno, Phys. Rev. B **70**, 153106 (2004).
[42] Z. V. Pchelkina, I. A. Nekrasov, T. Pruschke, A. Sekiyama, S. Suga, V. I. Anisimov, and D. Vollhardt, Phys. Rev. B **75**, 035122 (2007).
[43] D. J. Singh, Phys. Rev. B **77**, 046101 (2008).
[44] Z. V. Pchelkina, I. A. Nekrasov, T. Pruschke, S. Suga, V. I. Anisimov, and D. Vollhardt, Phys. Rev. B **77**, 046102 (2008).
[45] A. Damascelli, D. H. Lu, K. M. Shen, N. P. Armitage, F. Ronning, D. L. Feng, C. Kim, Z.-X. Shen, T. Kimura, Y. Tokura, Z. Q. Mao, and Y. Maeno, Phys. Rev. Lett. **85**, 5194 (2000).
[46] A. P. Mackenzie, S. R. Julian, A. J. Diver, G. J. McMullan, M. P. Ray, G. G. Lonzarich, Y. Maeno, S. Nishizaki, and T. Fujita, Phys. Rev. Lett. **76**, 3786 (1996).
[47] C. Bergemann, A. P. Mackenzie, S. R. Julian, D. Forsythe, and E. Ohmichi, Adv. Phys. **52**, 639 (2003).
[48] D. J. Singh, Phys. Rev. B **52**, 1358 (1995).
[49] T. Oguchi, Phys. Rev. B **51**, 1385 (1995).
[50] M. Braden, Y. Sidis, P. Bourges, P. Pfeuty, J. Kulda, Z. Mao, and Y. Maeno, Phys. Rev. B **66**, 064522 (2002).
[51] A. T. Rømer, I. Eremin, P. J. Hirschfeld, and B. M. Andersen, Phys. Rev. B **93**, 174519 (2016).